



In situ acoustic characterization of a porous layer backed by a large air cavity

Baltazar Briere de La Hossieraye^{1,a}, Jieun Yang^{1,b}, Maarten Hornikx^{1,c}

¹Department of the Built Environment, Eindhoven University of Technology, P.O. Box 513, 5600 MB, The Netherlands
{^a b.g.j.briere.de.la.hossieraye@tue.nl, ^b j.yang3@tue.nl, ^c m.c.j.hornikx@tue.nl }

Abstract

The *in situ* characterization of acoustic surfaces is a crucial challenge in room acoustics, as laboratory measurements of mounted materials are difficult to be arranged. In previous work, an approach to characterize locally reacting porous samples backed by a hard wall was studied and showed good accuracy. However, when a porous layer is backed by a large air cavity (depth > 100 mm), a configuration typically found in suspended ceilings, the air cavity features a non-locally reacting behaviour; thus the local reaction cannot be assumed safely.

This work presents a procedure to characterize such a non-locally reacting system by *in situ* PU probe measurements, where the non-acoustical parameters of the system are retrieved by a model-fitting approach comparing the measured complex reflection coefficient to the one of a porous layer without backing. The procedure was applied to 9 combinations of 3 porous layers backed by 3 air cavity depths each. A good agreement was observed between the retrieved parameters and references values.

Keywords: *In situ* measurement, model fitting, PU probe, porous materials

1 Introduction

One of the most common problems met in room acoustic consultancy and research practice is to accurately evaluate the acoustical properties of materials installed in an existing room. It is especially crucial in the case where a room acoustic simulation of the existing room is to be done, as the correctness of material properties used as input has a large influence on the accuracy of the simulation [1]. In such cases, laboratory measurements which are typically conducted to obtain the acoustical properties of materials, such as the impedance tube method [2], are not feasible since it is rarely possible to take off the sample of material for a laboratory measurement. Furthermore, even in the event a duplicate sample can be obtained for laboratory measurements, the mounting conditions and the wear of time can still alter the acoustical properties, so that an *in situ* evaluation of the properties is required.

Significant research effort was made on *in situ* measurement and characterization of material properties. Many of these approaches are summarized in a review of *in situ* measurement techniques by Brandao et al. [3]. More recent works are presented in Refs. [4]-[7].

In previous work by the authors of this paper, it was shown that combining a pressure-velocity (PU) *in situ* measurement method with a model fitting allowed a fast and accurate characterization of a locally reacting porous material backed by a hard surface [8]. In the continuation of this work, the applicability of this approach to other types of common acoustic systems is investigated.

Among the sound-absorbing systems commonly encountered in practice, porous layers backed by a large air cavity pose a challenge for such an approach of *in situ* characterization. Such systems are commonly found in the form of suspended ceilings, where an air cavity (100 - 500 mm) is present above the layer. In such conditions, the large air cavity behind the porous layer makes the system non-locally reacting, which hinders the results obtained by direct application of the method presented in our previous work. For such cases, an alternative procedure is needed for an accurate *in situ* characterization.

In this paper, an *in-situ* method is proposed to characterize a porous layer backed by a large air cavity. To overcome the challenge due to the non-locally reacting behaviour of the system, the fact that the properties of a porous layer with a large air cavity resemble the ones of a porous layer without backing is used. By using a model fitting procedure that finds minimal deviation between the measured reflection coefficients and predicted reflection coefficients based on an impedance model, the flow resistivity and the thickness of the porous layer will be retrieved. The depth of the cavity behind the layer is then retrieved from an analysis of the resonance frequencies in the complex reflection coefficient spectrum.

This paper is structured as follows: Section 2 presents the proposed characterization procedure in detail. Section 3 presents the methods used to validate the proposed method. In Section 4, the results of the characterization from virtual suspended ceilings (ideal cases) and real-life measurement are presented, along with an assessment of the resulting error in terms of acoustical properties. Finally, conclusions and prospects are discussed in Section 5.

2 Characterization procedure

The *in situ* characterization method proposed in this work follows the same general layout as the procedure described in Ref. [9]. It consists of two steps: a PU *in situ* measurement above the surface of the boundary system to characterize, and a post-processing that retrieves the non-acoustical parameters of the system based on a model-fitting procedure.

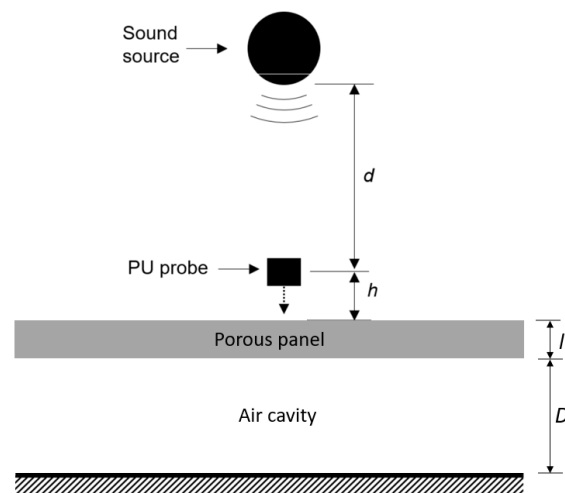


Figure 1 – Arrangement of the sound source and PU probe above a porous panel backed by an air cavity to measure Z_m .

2.1 Impulse response measurement

Impulse responses of the acoustic pressure and normal particle velocity are captured with a PU probe near the material's surface ($h < 20$ mm), as well as in free field, with a small sound source in vertical alignment with the probe at a distance $d = 260$ mm. The configuration used to measure the material's surface is pictured in Figure 1. After a time-windowing step with the Adrienne window [9] that allows the removal of late parasitic reflections, the impedance in free field Z_{ff} and near the material surface Z_m are computed from the measured impulse responses and the normal reflection coefficient is estimated as

$$R_{in\ situ}(h) = \frac{\frac{z_m}{z_{ff}} - 1}{\frac{z_m}{z_{ff}} \left(\frac{d}{d+2h} \right)^{\frac{(ik(d+2h)+1)}{ikd+1}} + 1} e^{ik2h}. \quad (1)$$

Equation (1) estimates the reflection coefficient under the assumption that both incident and reflected wave are plane waves but includes a correction for the amplitude decay of spherical propagation, which provides more accurate results for a short source-to-probe distance.

2.2 Estimation of the flow resistivity and thickness of the porous layer

The model fitting process to retrieve the porous layer parameters makes use of the normal incident plane wave reflection coefficient predicted for a porous layer without any hard backing (standalone porous layer: “air - porous layer – air” system). This model was chosen over the impedance model of a porous layer backed by an air cavity because the latter model’s is inaccurate when the air cavity depth is large. Furthermore, it was observed that in such a case, the global trend of the complex reflection coefficient resembles the one of the standalone porous layer. It will be shown in this paper that this allows retrieving the system’s properties with good accuracy.

The measured reflection coefficient is thus compared to the predicted reflection coefficient of a standalone porous layer, using the empirical Delany-Bazley-Miki (DBM) model. The DBM model predicts the characteristic impedance ξ_c (normalized with respect to the characteristic impedance of air) and propagation constant k_c of a porous medium from the flow resistivity σ with the following polynomial expressions

$$k_c(f, \sigma) = \frac{2\pi}{c_0} \left[1 + 7.81 \left(10^3 \frac{f}{\sigma} \right)^{-0.618} - j11.41 \left(10^3 \frac{f}{\sigma} \right)^{-0.618} \right], \quad (2)$$

$$\xi_c(f, \sigma) = \left[1 + 5.50 \left(10^3 \frac{f}{\sigma} \right)^{-0.632} - j8.43 \left(10^3 \frac{f}{\sigma} \right)^{-0.632} \right]. \quad (3)$$

The plane wave reflection coefficient of normal incident sound wave of the standalone porous layer with thickness l is then predicted following the transfer matrix formulation

$$R_{layer}(f, \sigma, l) = \frac{(\xi_c + 1)(\xi_c - 1)e^{i2k_c l} + (1 - \xi_c)(\xi_c + 1)}{(\xi_c + 1)(\xi_c + 1)e^{i2k_c l} + (1 - \xi_c)(\xi_c - 1)}. \quad (4)$$

Using the formulations from Equations (1) and (4), a cost function is set to minimize the difference between the measured data $R_{in-situ}(h)$ and the prediction $R_{layer}(\sigma, l)$ which becomes

$$F(\sigma, l, h) = \sum_{\Delta f} \left\| \text{Re}(R_{in-situ}(f, h) - R_{layer}(f, \sigma, l)) \right\| + \sum_{\Delta f} \left\| \text{Im}(R_{in-situ}(f, h) - R_{layer}(f, \sigma, l)) \right\| \quad (5)$$

where Δf is the frequency range of the fitting. The frequency range of interest in this work is $\Delta f = [1 - 8]$ kHz because this is where the plane wave assumption is the most accurate for the used experimental setup. The lower and upper bounds of the frequency range are f_l and f_u respectively. For the fittings performed in this work, the elements of the frequency vectors were logarithmically spaced to avoid a larger weight of the higher frequencies.

The cost function F is minimized in MATLAB with the *fmincon* function used as core solver to a *MultiStart* object, which runs the solver for a given number of starting points uniformly distributed across the search space, and yields the best minimum.

The search space, which is defined by the lower (x_l) and upper boundaries (x_u) for each parameter, is presented in Table 1. The search space of the flow resistivity (σ) is chosen to encompass the values encountered for the most commonly used porous materials. The probe-to-sample distance (h) is expected to be within [0,30] mm. It should be noted that the thickness of the material (l) is considered as a variable in the characterization process in the same manner as the flow resistivity. This simulates a scenario when it is not possible to measure the material thickness due to mounting conditions. Furthermore, the probe to sample distance h is also considered as a fitting variable, as its exact effective value is difficult to measure with sufficient precision. In this study, the probe was placed about 10 mm above the material.

The number of starting points chosen to run the *MultiStart* process is $N_s=50$, which ensured the finding of a unique optimum point in this search space. This was assessed with a normalized standard deviation lower than 1% over 7 *Multistart* runs for each parameter. For the fitting process, the data was reduced to 300 logarithmically spaced frequencies.

The parameters yielding the best fitting (named hereafter σ^* , l^* and h^*) are then used for the final estimations of the measured and DBM-fitted reflection coefficients as follows

$$R_{in-situ,opt}(f) = R_{in-situ}(f, h^*) \quad (6)$$

$$R_{layer,opt}(f) = R_{layer}(f, \sigma^*, l^*) \quad (7)$$

Table 1 – Lower (x_l) and upper limits (x_u) of search space for the optimization variables in this study.

	x_l	x_u
σ (kPa s/m ²)	1×10^3	1×10^6
l (mm)	0	200
h (mm)	0	30

2.3 Estimation of the air cavity depth

Once the previously described model fitting is done, estimations of the porous layer thickness l^* and flow resistivity σ^* are obtained. In case an *in situ* inspection is not possible, the air cavity depth behind the sample still needs to be retrieved.

The proposed method estimates the air cavity depth by analysis of the resonance peaks in the measured reflections coefficient, using the previously estimated porous layer thickness

$$D^* = \frac{c_0}{2\delta_f} - l^* \quad (8)$$

$$\delta_f = \sum_{n=1}^{N-1} \frac{f_{n+1} - f_n}{N-1} \quad (9)$$

In Equation (9), the f_n is the n^{th} peak frequencies, and N is the total number of detected peaks.

This method to estimate the cavity depth implicitly assumes that the travelling time of the sound wave in the porous material is negligible compared to the travelling time of the sound wave in the air cavity, which is true in most cases if the porous layer is thin compared to the cavity depth. The average over the frequency leaps between consecutive peaks is used to mitigate the error related to the variation of the sound speed with frequency in the porous layer.

The peak detection was performed with the *findpeaks* function in MATLAB, applied to the real part of $R_{in-situ,opt}$. It is also possible to detect the interference peak visually from the measurement spectrum, the latter method being preferred in case of a noisy signal, because in such case parasitic peaks are likely to be detected irrelevantly.

3 Experimental validation

The experimental validation of the procedure was performed on three porous layers (materials A, B and C), that were mounted above a concrete floor with three cavity depths: 160 mm, 240 mm and 500 mm. The dimensions of the samples were 500×500 mm for materials A and B, and 600×1000 mm for material C. These dimensions were considered sufficient to avoid significant size effects above 1 kHz, which is the frequency range measured. The reference flow resistivities and thicknesses of the three samples are shown in Table 2.

Table 2 – Reference flow resistivities and thicknesses of the porous layers used for the experimental validation. The flow resistivities values were obtained from impedance tube measurement using the low frequency limit of the dynamic mass density [11].

Sample	σ_{ref} (kPa s/m ²)	l_{ref} (mm)
Material A	33	20
Material B	30	40
Material C	13	60

The measurements were realised with the "In situ absorption testing" (name by the manufacturer, Microflown Technologies). It consists of a PU probe attached to a small round loudspeaker via a light decoupling structure, which sets the source-to-probe distance to 260 mm. The source signal, a 5 seconds e-sweep sine, was produced from a laptop running the room acoustic software DIRAC 6. The signal was sent to an amplifier before being sent to the small source. The acquired signals were recorded by the same laptop and the de-convolutions into impulse responses were performed by DIRAC 6.

The setup was positioned close to the panel's surface with the help of a tripod, so that the probe was located at a height $h_{ref} = 10$ mm above the surface and the source vertically aligned with the probe, as shown in Figure 2. The velocity sensor was carefully oriented to capture the velocity normal to the sample's surface. As for the horizontal location above the plane, the PU probe was placed within the confidence region for PU probe measurements, which minimizes the influence of the sound waves diffracted on the edges of the samples [10]. This means that the probe was placed within a distance of $L/3$ from the center of the sample, with L being the side length of the sample. Additionally, care was taken to not place the probe exactly at the centre of the sample, where edge-diffracted waves interfere constructively.



Figure 2 – Picture of the experimental validation setup. The sample of material B is mounted on rubber bars to create a 240 mm air gap between the sample and the concrete.

The area within 1 m around the measurement location was cleared to avoid strong parasitic reflections from neighbouring objects. By doing so, the time windowing of the impulse responses can be chosen so as to include the reflection from the concrete floor in the largest air gap configuration (500 mm), while windowing out the later reflections from the neighbouring environment. These considerations led to the use of an Adrienne windows with a total time length of 6 ms for the time-windowing of the impulse responses.

4 Results

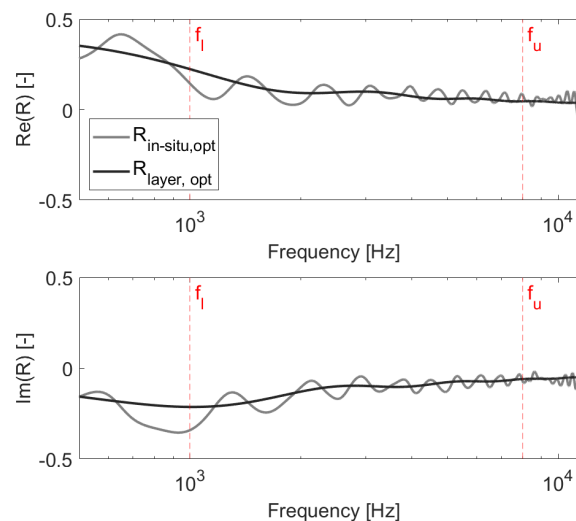


Figure 3 – Comparison of measured reflection coefficient (Material C with a 160 mm cavity) and fitted model of standalone layer. A similar global trend within the fitting frequency range (delimited with red lines) is observed between case with the air cavity, which is measured ($R_{in-situ,opt}$), and the case without backing, which is modelled and fitted to the measurement ($R_{layer,opt}$).

The characterization results of the experiment are shown in Table 3, and an example of the obtained fitting is pictured in Figure 3. For each configuration measured, the optimal parameters σ^* , l^* and h^* are presented, as well as the estimated cavity depth D^* . It can be observed that the values retrieved for the flow resistivity

vary significantly depending on the air cavity depth behind the sample, with the error to the reference value being greater for a larger air cavity. A possible reason for this is that the flow resistivity has a reduced influence on the measured acoustical properties as the air cavity becomes larger. Because of this reduced influence, retrieving the flow resistivity through the model fitting of the acoustical properties becomes less accurate.

The retrieved thickness are however in good agreement with the references, with a maximum observed deviation of 15% (Material B with 240 mm cavity). The retrieved cavity depths are also in very good agreement with the reference, with deviations lower than 8%. In terms of absolute values, it can be noted that the deviations observed correspond at most to a 6 mm error for the porous layer thickness and to a 19 mm difference for the cavity depth.

It can also be seen that the retrieved values for the probe-to-sample distance are always within a 3 mm deviation to the measured distance (10 mm), which suggests that using h as a fitting variable leads to realistic results and does not hinder the characterization.

To investigate the influence of the characterization error on the modelling of the acoustic properties, the normal incidence absorption coefficient was computed in 1/3 octave bands from the retrieved parameters and compared to the absorption coefficient obtained from the reference parameters. This can be seen in Figures 4, 5 and 6 for materials A, B and C respectively, in the frequency range 80 Hz - 12 kHz. The maximum errors for each case are reported in Table 4.

It can be seen from the figures that the reconstructed absorption coefficients are in very good agreement with the references for all the measured systems. In most of the measured cases, the error in 1/3 octave band appears negligible. For some cases, such as Material B with 240 mm cavity (Figure 5 (b)) and Material C with 500 mm cavity (Figure 6 (c)), visible errors are however observed in the lower 1/3 octave bands.

From Table 4, the maximum error observed in the absorption coefficient is 0.13, which is obtained for material C backed with a 500 mm thick cavity. For all the other cases, the maximum error remains below 0.10 (or $0.10 \times \pi$ of phase error). It appears from this result that a combination of a low flow resistivity layer with such a large air cavity is unfavourable to predict the acoustical properties accurately.

These results suggest that the *in situ* characterization procedure provides a prediction of the acoustic absorption of the system that is in good agreement with the prediction obtained from the reference parameters.

Table 3 – Characterization results of measured samples. The relative errors (in %) to the reference are shown in parenthesis.

		D = 160 mm	D = 240 mm	D = 500 mm
Material A	σ^* (kPa s/m ²)	35 (+6%)	36 (+9%)	41 (+24%)
	l^* (mm)	20.5 (+3%)	22 (+10%)	22 (+10%)
	h^* (mm)	11 (+10%)	10.9 (+9%)	12.2 (+22%)
	D^* (mm)	156 (-3%)	240 (0%)	506 (+1%)
Material B	σ^* (kPa s/m ²)	31 (+3%)	28 (-7%)	36 (+20%)
	l^* (mm)	35 (-13%)	34 (-15%)	37 (-8%)
	h^* (mm)	10.4 (+4%)	9.7 (-3%)	12.0 (+20%)
	D^* (mm)	172 (+8%)	236 (-2%)	481 (-4%)
Material C	σ^* (kPa s/m ²)	13.0 (0%)	11.0 (-15%)	9.4 (-30%)
	l^* (mm)	52 (-13%)	59 (-2%)	57 (-5%)
	h^* (mm)	12.1 (+21%)	9.7 (-3%)	12.0 (+20%)
	D^* (mm)	165 (+3%)	254 (+6%)	489 (-2%)

Table 4 – Maximum error of the reconstructed acoustical properties to the reference, computed in 1/3-octave bands.

	Material A			Material B			Material C		
	$\varepsilon(R)$	$\varepsilon(\varphi(R))/\pi$	$\varepsilon(\alpha)$	$\varepsilon(R)$	$\varepsilon(\varphi(R))/\pi$	$\varepsilon(\alpha)$	$\varepsilon(R)$	$\varepsilon(\varphi(R))/\pi$	$\varepsilon(\alpha)$
D = 160mm	0.05	0.03	0.04	0.05	0.04	0.06	0.10	0.07	0.06
D = 240 mm	0.08	0.06	0.04	0.13	0.05	0.07	0.08	0.09	0.08
D = 500 mm	0.08	0.06	0.07	0.09	0.04	0.05	0.13	0.11	0.13

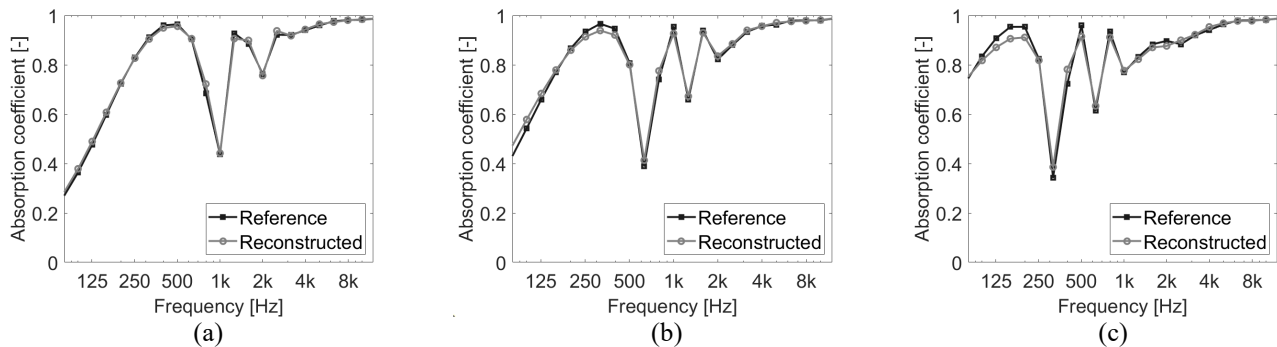


Figure 4 – Reference and reconstructed absorption coefficients of the porous layer backed by an air cavity (normal incidence) featuring material A with different cavity depths: 160 mm (a), 240 mm (b), 500 mm (c).

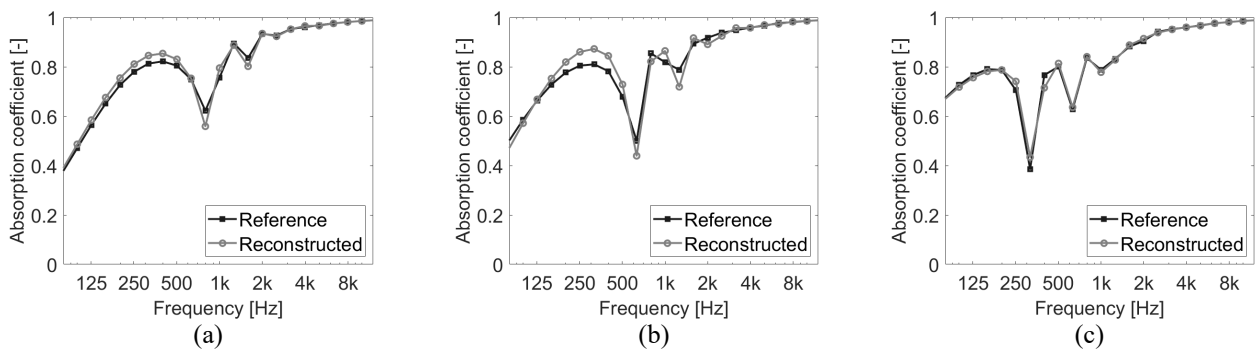


Figure 5 – Reference and reconstructed absorption coefficients of the porous layer backed by an air cavity (normal incidence) featuring material B with different cavity depths: 160 mm (a), 240 mm (b), 500 mm (c).

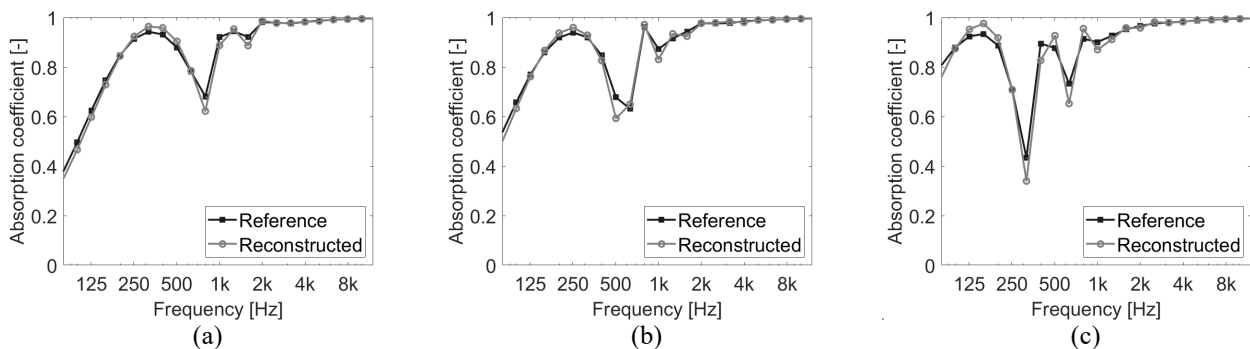


Figure 6 – Reference and reconstructed absorption coefficients of the porous layer backed by an air cavity (normal incidence) featuring material C with different cavity depths: 160 mm (a), 240 mm (b), 500 mm (c).

5 Conclusion

In this work, a method to *in situ* characterize a porous panel backed by a large air cavity is proposed. It consists of PU probe measurement, followed by a model-fitting procedure and a resonance analysis.

The procedure was used to characterize 9 combinations of porous layers backed by air cavities.

Experimental results show that the method allows an accurate estimation of the porous layer thickness and cavity depth, the maximum deviation being around 15%. Greater deviations, up to 30% were observed for the retrieved flow resistivity. This flow resistivity error was observed to increase with the air cavity depth of the measured system, regardless of the porous layer used.

Despite these deviations in retrieved parameters, the error in terms of predicted absorption coefficient, which was computed in 1/3 octave bands for normal plane wave incidence, remained small in all cases measured. The maximum error was observed about 0.13, and all the significant errors were found below the 500 Hz octave band. This result suggests that the proposed method to characterize suspended ceiling systems leads to accurate estimation of the acoustic properties, especially in the high-frequency region.

A natural continuation of this work is the characterization of coated porous materials, as most commercially available acoustic materials (wall absorbers or ceiling tiles) are covered with fabric.

Acknowledgements

This project has received funding from the European Union's Horizon 2020 research and innovation programme under the Marie Skłodowska-Curie grant agreement number 721536.

References

- [1] M. Vorlander. Computer simulations in room acoustics: Concepts and uncertainties. *The Journal of the Acoustical Society of America*, 133(3):1203–1213, 2013.
- [2] *ISO 10534-2, Acoustics Determination of sound absorption coefficient and impedance in impedance tubes Part 2: Transfer-function method*. International Organization for Standardization, Geneva, Switzerland, 1998.
- [3] E. Brandao, A. Lenzi, and S. Paul. A review of the in-situ impedance and sound absorption measurement techniques. *Acta Acustica united with Acustica*, 101(3):443–463, 2015.
- [4] M. Li, W. Van Keulen, E. Tijs, M. Van De Ven, and A. Molenaar. Sound absorption measurement of road surface with in-situ technology. *Applied Acoustics*, 88:12–21, 2015.
- [5] Nolan. Estimation of angle-dependent absorption coefficients from spatially distributed in situ measurements. *The Journal of the Acoustical Society of America*, 147(2):EL119–EL124, 2020.
- [6] M. Ottink, J. Brunskog, C.-H. Jeong, E. Fernandez-Grande, P. Trojgaard, and E. Tiana-Roig. In situ measurements of the oblique incidence sound absorption coefficient for finite sized absorbers. *The Journal of the Acoustical Society of America*, 139(1):41–52, 2016.
- [7] A. Richard, E. Fernandez-Grande, J. Brunskog, and C.-H. Jeong. Estimation of surface impedance at oblique incidence based on sparse array processing. *The Journal of the Acoustical Society of America*, 141(6):4115–4125, 2017.
- [8] B. Briere, D. L. Hosseraye, and M. Hornikx. Broadband Acoustic Material Characterization by Means of in-Situ Measurements and Impedance Model Fitting. *Forum Acusticum 2020*, pages 115–121, 2020.
- [9] M. Garai, P. Guidorzi, European methodology for testing the airborne sound insulation characteristics of noise barriers *in situ*: Experimental verification and comparison with laboratory data. *The Journal of the Acoustical Society of America* 108 (3), 2000.

- [10] E. Brandao, A. Lenzi, J. Cordioli. Estimation and minimization of errors caused by sample size effect in the measurement of the normal absorption coefficient of a locally reactive surface. *Applied Acoustics* 73 (6-7):543-556, 2012
- [11] L. Jaouen, E. Gourdon, P. Glé, Estimation of all six parameters of Johnson-Champoux-Allard-Lafarge model for acoustical porous materials from impedance tube measurements, *The Journal of the Acoustical Society of America* 148, 2020